

## Supplementary Materials: Optimization method

The parameters of the primitive cell were optimized as follows:

At a given frequency of 150 THz, the lattice period  $a$ , the thicknesses of silicon and silicon dioxide layers  $h_{\text{Si}}$  and  $h_{\text{SiO}_2}$ , the radius of the dielectric resonator  $b$ , and the thickness of the metamaterial layer  $h_{\text{MM}}$  were varied to achieve a high contrast between forward and backward transmission. For optimization, we used a combination of Monte-Carlo and gradient descend methods. Then, the selected combinations of parameters were studied in the frequency range around 150 THz.

Figure S1 shows the results of the parametric optimization. It can be seen that there are two distinct zones in the parametric space of  $a$ ,  $h_{\text{MM}}$ , and  $b$ , where the probability of finding a large difference between forward and backward transmission coefficients is higher. However, this difference is not continuous at scales larger than several tens of nanometers, meaning that the transmission contrast in the forward and backward directions changes very rapidly as a function of any dimensional parameter of the metasurface unit cell. This trend is even more pronounced in Fig. 2(b), where no pattern is observed in the dependence of the optimization function on the respective layer thicknesses. This particularity rendered the use of the gradient descend method ineffective at large scales in the parametric space. As a result, the only viable method appeared to be the Monte-Carlo method. After applying it, several particular points in the parametric space were selected for further studies. Firstly, these points were locally optimized by the gradient descend method. Secondly, they were studied in the extended frequency range near 150 THz. Two of these points were chosen as representative of general trends.

Points 1 and 2 maximize the difference between the forward and backward transmission over the whole set of simulations performed. It should be noted that we cannot claim that points 1 and 2 represent the absolute maximum of this difference. Indeed, because of the discontinuities of the optimization function in the parametric space, as well as the very poor convergence of the algorithm at some points, it is practically impossible to find the global maximum of the optimization function.

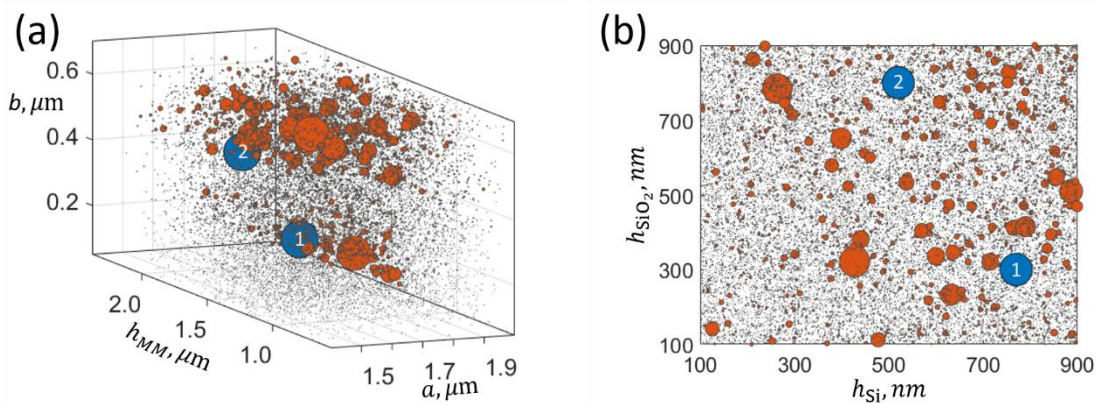


Fig. S1. Results of parametric optimization in the parametric space of lattice period  $a$ , metamaterial thickness  $h_{\text{MM}}$ , and meta-atom radius  $b$  (a), and in the parametric space of silicon and silicon oxide layer thicknesses,  $h_{\text{Si}}$  and  $h_{\text{SiO}_2}$  (b). Each circle on the diagram represents the simulated combination of parameters, and its diameter corresponds to the absolute value of the difference between the transmission in the forward and backward directions. The blue circles (1) and (2) represent the parameter combinations used for the simulations, the results of which are shown in Figs. 3 and 4 of the article, respectively.

## Supplementary Materials: Multipole decomposition

Figure S2 shows the multipole decomposition of the modes excited in linear regime in the systems shown in Figs. 2 and 3 of the main text, which will be further referred to as System 1 and System 2, respectively. Firstly, it is evident that the excited modes differ significantly from purely dipolar excitations. Moreover, while the excitations in System 1 are predominantly dipolar, the excitations in System 2 show a much richer multipole composition. This can be explained by the fact that the cylinder radius in System 2 is larger with respect to the wavelength. Secondly, the decomposition confirms the hypothesis that the asymmetry in the excitation of multipoles is responsible for the non-reciprocal transmission in the presence of nonlinearity. It is clearly visible that the partial multipole cross-section can differ significantly for forward and backward illumination. It should be noted, however, that the total extinction cross-section does not depend on the direction of illumination in the linear regime.

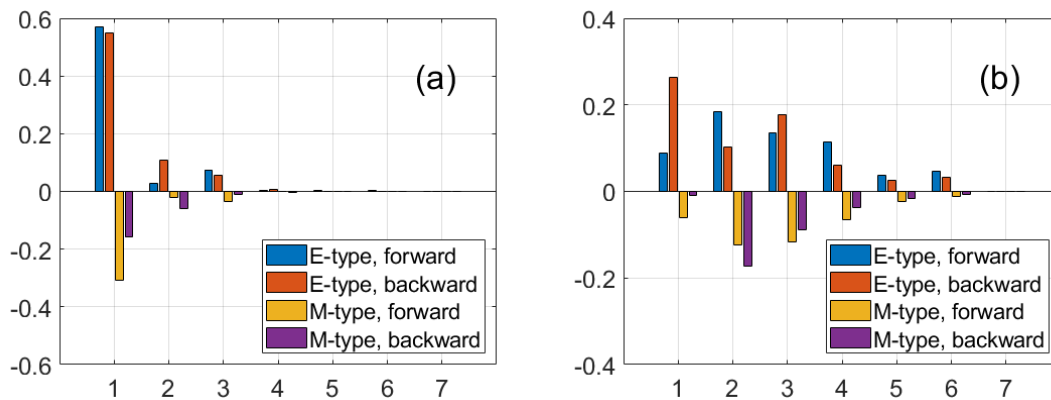


Fig. S2. Multipole decomposition of the electromagnetic modes excited in System 1 (a) and System 2 (b). The partial multipole cross-sections are normalized with respect to the total extinction cross-section, such that the sum of all partial cross-sections is equal to 1. The x-axis represents the order of the multipole: 1 corresponds to dipole, 2 – to quadrupole, 3 – to octupole, etc.